

PCB Integration of Dye-sensitised Solar Cells for Internet of Things Applications

Jens Eliasson*, Jerker Delsing*, Simon J. Thompson†, Yi-Bing Cheng†, and Peter Chen‡

*Dept. of Computer science, space and electrical engineering
Luleå University of Technology, SE-971 87 Luleå, Sweden
Email: jens.eliasson@ltu.se

†Dept. of Materials Engineering, Monash University, Melbourne, Australia
Email: yibing.cheng@monash.edu

‡Dept. of Photonics, National Cheng Kung University, Tainan, Taiwan
Email: petercyc@mail.ncku.edu.tw

Abstract—Internet of Things is envisioned to drastically change the way sensor data from physical phenomena can be utilized by users on the Internet. However, one concern in deploying and maintaining a large number of sensor nodes is that replacing spent batteries will not be feasible. One solution to this issue may involve utilising energy harvesting technologies, e.g. solar, heat, or vibration, with solar being the most promising for general applications. However, using solar panels is currently a relatively expensive approach as they require a time-consuming and therefore costly assembly process. As an alternative, this paper suggests a new approach to powering networked sensors: the direct integration of a solar cell onto a sensor nodes printed circuit board. This approach eliminates the need for manual assembly and the use of expensive connectors.

Keywords-Dye sensitised solar cells, energy harvesting, Internet of Things, wireless sensor networks

I. INTRODUCTION

This paper, based on previous work from Eliasson et al. [1], presents new results and outlines application areas for the proposed approach. A wireless sensor and actuator network (WSAN) is composed of a large number of heterogeneous sensor nodes, or *sources*, that both sense phenomena in the physical world but also provide some control of the physical world [2]. A wireless sensor and actuator network also includes one or several gateways, or *sinks*, which forward sensor data from nodes in the internal network to an external network [3]. Research on WSAN technology originally focused on military applications, such as battlefield surveillance, land

mine detection, and soldier monitoring [4]. Current wireless sensor network research is additionally motivated by an increasing number of civil usage scenarios, such as environmental and habitat monitoring, seismic and volcanic monitoring, structural monitoring, and industrial applications [5], [6].

Wireless sensors are expected to have a drastic impact on how measurements of the physical world will be presented to users on the Internet [7]. A vision, in which Internet-connected wireless sensors are deployed in the vicinity of users, named *the Internet of Things* [8] is also projected to enhance both safety and quality of life for future generations. For this vision to be realized, a number of issues must be resolved. Two of these issues, addressed by this paper, are:

- Enabling wireless power
- Lowering the cost of the sensor nodes

Reducing power consumption can be achieved using a number of methods, such as using more efficient components, integrating more intelligent routing protocols [9], or developing energy-aware computing. Wireless power requires power harvesting, power storage, and an appropriate power usage architecture at the sensor node; see for example [10], [11], [12]. A node's cost will be reduced with the use of more integrated components, and the price of printed circuit boards (PCB), integrated circuits (ICs), and other components will drastically decrease with increased production volumes. However, the costs of certain node components, such

as batteries and power supplies, do not scale as effectively as circuit board production volumes. The cost of packaging a complete node with a circuit board, batteries, solar panels, and enclosure will not be reduced by the same order of magnitude as that of the electronics. This is a major obstacle for realizing the vision of massive wireless sensor networks.

This paper presents a novel approach aimed at further reducing manufacturing and integration cost for solar cells for powering wireless sensor nodes. The approach is to manufacture a solar panel directly onto a sensor node's circuit board, thus reducing the cost of manufacturing the cell separately and eliminating the assembly cost. This has several benefits, as the resulting device consists of an integrated solution that effectively eliminates cables and connectors, and an additional integration step. The proposed approach also increases the system's robustness because there are no connectors or cables that can disconnect due to mechanical phenomena, e.g., vibrations or impacts. The ultimate aim of this research is to develop a holistic method for producing complete low-power systems, where assembly of the PCB, components, and an energy-harvesting device can be completed as a single process. The first steps have been taken - we have integrated a solar cell module with a PCB - and the authors envision that, in the future, a solar cell can be directly printed on a PCB using sequential build-up (SBU) techniques. For example, Blackshear et al. reported in 2005 [13] the advantages of using SBU for chip assembly onto circuit boards.

The paper is outlined as follows: this section has presented related work and a background of wireless sensor networks and solar cell technologies. The next two sections give an overview of some related work, application areas, and DSCs. Section V presents the new method of integrating a DSC directly onto a circuit board, and Sections VI and VII show the experimental setup, and results from real-world tests, respectively. Finally, conclusions and suggestions for future work are presented in Section VIII.

II. RELATED WORK

One consideration for energy harvesting relates to the energy density from different sources. It is clear that solar cells are superior to other energy

harvesting approaches such as vibrations and thermoelectric power, as reported by Yang et. al [10]. When comparing different solar cell technologies, both power efficiency and cost must be considered. Two main candidate technologies: silicon based solar cells and dye sensitised solar cells (DSC), sometimes called Grätzel cells [14], have been selected for further investigation. A comparison between silicon based solar cells and DSC can be found in [15]. Regarding energy capability a traditional silicon-based solar cell offers about $43mA/cm^2$ at 0.7V, whereas current DSCs offer about $22mA/cm^2$ at about 0.6V [16]. Regarding cost, DSCs have potential to be lower cost due both cheaper feedin materials and inexpensive manufacturing techniques.

In [17], Usman showed by simulation that the use of DSC technology in close integration with modern electronics, i.e. PCB integration, is an interesting technology and emerging trend. In [1], Eliasson et al. showed the world's first working prototype of a device where a PCB and a DSC cell was successfully integrated. This paper further elaborates on application areas where this is feasible, and extends the conclusions by supplying new measurements and results.

III. AREAS OF APPLICATION OF PROPOSED APPROACH

The use of energy scavenging in real-world applications is becoming more and more common. By harvesting energy in the form of solar, wind, vibration, heat, etc, the need to replace or charge drained batteries can be avoided. In some cases, for example industrial applications, changing batteries might not be feasible due to a hazardous environment. Below are three different sensor networking applications identified, with their characteristics:

A. ITS

Intelligent transport systems (ITS) are believed to be an important tool for tomorrow's road infrastructures. ITS can help reducing the traffic's carbon dioxide foot print, improve safety and increase the traffic flow. ITS systems are usually composed of three main components: sensors for vehicle detection, actuators for informing drivers, and a back-end system. Sensors for vehicle detection are used to feed the back-end system with information about the traffic, with number of vehicles, thier speed, etc.

Vehicle detection has traditionally been performed using magnetic sensors, cameras, lasers and other expensive and power consuming devices. A road surface network (RSN) is a new type of ITS solution, where low-cost sensors are deployed directly onto a road's surface. This enables vehicle detection and classification, not only in cities, but also in rural areas. Since the sensors are solar-powered, there is no need for installing power cables, which further reduces the installation cost. The use of a wireless sensor and actuator network (WSAN), as suggested by Hostettler et al. [18] enables new possibilities of how modern, solar-powered electronics can be embedded in the physical world. The iRoad project [19] conducted at Luleå University of Technology aims at developing these types of systems. In these types of devices, it is important that both component and assembly costs are minimized.

B. Healthcare

Most western countries have an aging population. This will drastically increase costs for each country's healthcare and elderly care systems. Using for example e-Health, where electronics and ITS systems [20] are used as tools for reducing healthcare costs, travel costs and increase the quality of life. With e-Health, people which can be treated in the comfort of their own homes can have the option to do so, thus minimizing hospital time. However, this requires that some sort of monitoring be used. With the use of (wireless) sensors, patients can have their medical status monitored remotely while maintaining mobility, and if some anomaly is detected by an e-Health device, an alarm or alert can be transmitted to the hospital. Figure 2 shows an example of an Internet-connected sensor platform, i.e. the Mulle. The Mulle is a low-power sensor node, measuring only 24x26x4 mm. This small size combined with the Mulle's support for Internet communication, enables the Mulle to be well suited for use on patients or elderly. The Mulle can be equipped with GPS, heart rate monitor, fall sensors, motion sensors and other types of sensors that can be used to monitor patients. Figure 1 shows a Body area network (BAN) architecture capable of monitoring various medical properties such as body temperature, posture, pulse, location, physical activity, etc. A number of sensor nodes would be deployed on a human user, and use the patients mobile

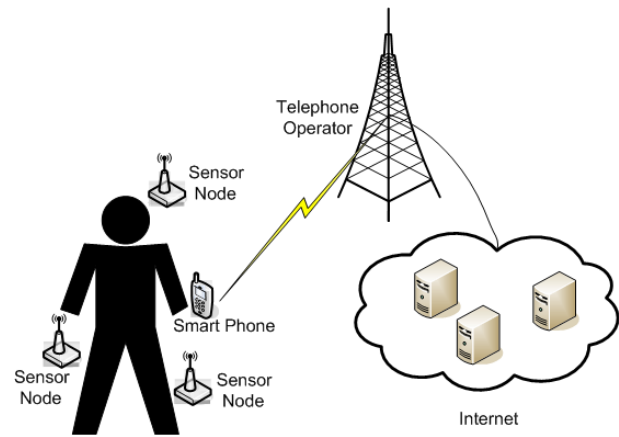


Fig. 1. Body area network

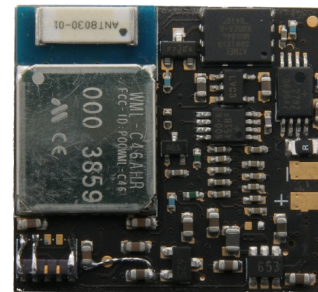


Fig. 2. Mulle v3.1 Embedded Internet System (EIS)

phone to transmit sensor information to backend-systems for data analysis and alarm generation.

In e-Health applications, users expect not to change drained batteries more than a few times per year. If an e-Health device must be recharged daily or weekly, people will simply not use it, or forget to charge it resulting a health hazard. Therefore, e-Health devices must be very low power, and optionally use energy scavenging in order to prolong system lifetime. The Mulle's sleep current consumption is only 4 μA , which enables it to be used in combination with (solar) energy scavenging, as shown in [12].

One aspect of e-Health applications is that the users will spend a substantial time indoors. It is therefore beneficial if the solar panel used to power the sensor and actuator devices can provide some power output even in low light conditions i.e. from lamps and ambient sun light.

C. Home automation

Home automation using wireless sensor and actuator networks have the possibility to reduce energy

usage [21] and thus CO₂ emissions [22], increase safety and security while enhancing the users quality of life. By enabling different systems to exchange information and thus allow fine control of heating, ventilation, lighting etc, substantial savings can be accomplished. As an example, the building's security system can inform other systems that no one is present. Heating and ventilation can then be reduced, lighting switched off etc. Temperature sensors outdoors and indoors can help ensure that a comfortable temperature is provided in each individual room. Smart appliances, such as washing machines, can start during night when the electricity is cheap.

IV. DYE SENSITISED SOLAR CELLS

The dye sensitised solar cell (DSC) is currently being investigated as a low cost method of harvesting the abundant energy of sunlight into electricity [14]. It offers the possible advantages of low cost and better light harvesting in low and/or diffuse lighting, which are more realistic conditions than those which are optimal for other photovoltaic devices, such as silicon-based cells.

The DSC operates by light exciting an electron in a dye molecule adsorbed onto a mesoporous semiconductor to an energy level above the conduction band of the semiconductor. The electron is quickly transferred to the conduction band of the semiconductor and transported through the network of interconnected nanoparticles to the electrode. The electron passes through the external circuit and then reduces an electrolyte at the counter electrode which in turn reduces the dye, returning it to its ground state. This type of solar cell has exhibited an efficiency of over 11 %, as shown by Han et. al [23]. The operation of the DSC allows for cheap, abundant materials to be used for device components, combined with less energy-intensive processes used during manufacture. This offers the potential for significantly lower production costs compared to more traditional silicon solar cells, in turn reducing the energy and cost payback times significantly. These factors make the DSC an attractive renewable energy source for the future.

The drawbacks for DSCs are, lower performance compared to silicon devices and a corrosive volatile electrolyte that limits material selection options and shortens device lifetimes. The most problematic of

these is device lifetime, as it is difficult to construct devices with long lifetimes when encapsulation of a volatile, corrosive electrolyte is required. To this end alternative electrolytes have been investigated - generally highly viscous, non-volatile ionic liquids. Solid state hole conductors have also been considered and are a more elegant solution, as they also remove corrosive iodine from the system, expanding materials selection options within the cell as well as eliminating any solvent leakage issues, due to being a solid. The leading organic hole conductor is 2,2,7,7-tetrakis(N,N-di-p-methoxyphenyl-amine)-9,9-spirobifluorene (spiro-MeOTAD) [24], with reported device efficiencies up to 7.2% [25]. A solid state device is typically constructed onto fluorine doped tin oxide (FTO) glass with a titania (TiO₂) layer coated on top, which is dyed and then infiltrated with the hole conductor. The counter electrode is a gold layer evaporated onto the coated titania layer and connected to an electrically isolated section of the FTO glass. This architecture is ideal for integration with circuit boards, which has been realised by the authors and is shown in Figure 3. The circuit board was physically contacted to the gold contacts on the back of the DSC module, as shown in Figure 5. The connections was made such that each cell is independently measurable and thus can be bypassed if necessary, e.g. due to damage or during cell characterization.

V. PCB WITH INTEGRATED DYE SENSITISED SOLAR CELL

DSC modules were created here using the screen printing technique, on pre-etched 100 mm × 100 mm 13 Ω/square FTO coated conducting glass (Nippon) masterplates. The etching to separate the contacts for the individual cells was performed using a laser engraving system, a Versa laser VL3.50 unit, which produced fine lines (~150 μm) with high spacial precision. Following this procedure the glass was cleaned and a dense blocking layer of TiO₂ was deposited by spray pyrolysis, with the areas for electrical contacts by solder or the gold layer being masked by flattened aluminum rods.

The screen printing paste for the active layer contained 18 nm particles of anatase titania (obtained from JGC Catalysts and Chemicals Ltd) and was diluted by terpineol at a ratio of 2:1 paste (Fluka). The thickness of the titania layer was determined

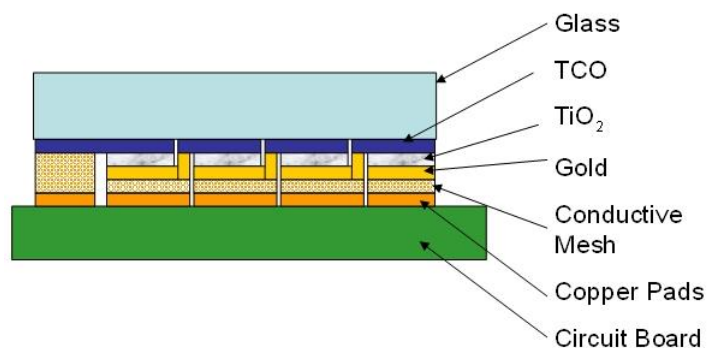


Fig. 3. Layout of the PCB with integrated dye-sensitised solar cell

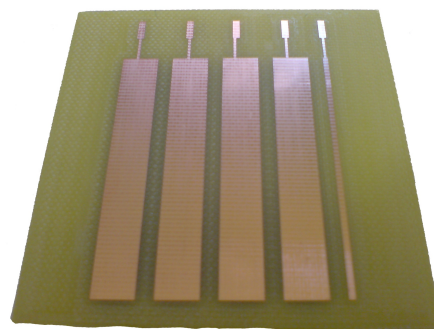
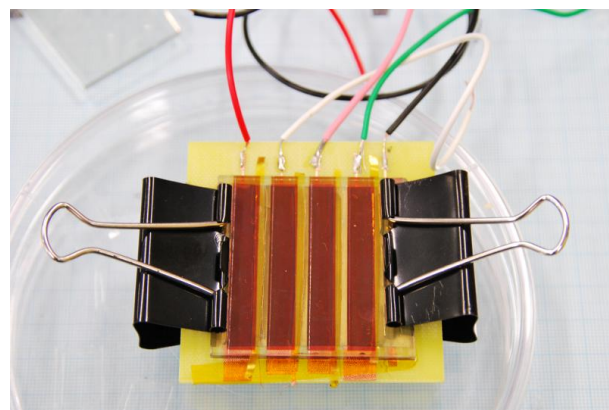


Fig. 4. Prototype board layout

by a Veeco Detak 150 stylus profilometer, to be ~ 2 μm . The titania layer was incrementally heated to 450°C for 30 min and then to 500°C for 15 min. The master plates were cut into $50\text{ mm} \times 50\text{ mm}$ modules and reheated to 500°C for 30 mins before being placed into the dye solution of 30 mM Z907 (Dyesol) in an acetonitrile/tert-butanol 1:1 mixture, for approximately 24 hours. The electrolyte was a solid state hole conductor, namely Spiro-MeOTAD, which was deposited by spin-coating using a solution that consisted of 180mg/mL of Spiro-MeOTAD (Merck) in chlorobenzene (Sigma) with additives of 4-tertbutylpyridine (TBP) (Sigma) (17.6ul/mL) and Li-TFSI (Sigma) (19.5mM). Chlorobenzene was used on a cotton bud to remove excess Spiro-MeOTAD from the glass were series interconnects were to be formed. The gold charge collecting layer was deposited onto the module via thermal evaporation, and the areas not to be coated with gold were masked with Kapton tapeTM (3M).

An attempt was made to integrate these devices onto a PCB using conductive epoxy however, this had a detrimental effect on the DSC leading to dye desorption. Therefore, this approach was abandoned in favour of using a soft compressible conductor. The material used was a polymer mesh substrate with copper deposited onto it. The copper mesh was cut into pieces of the same width as the pads, but slightly longer such that they could be laid over the pads and adhered using Kapton tape. The module was placed on top of the PCB such that the gold contacted the copper mesh and no shorting occurred between cells. The PCB and DSC module were then clipped into place using bulldog clips. During these alignment and clipping processes care was taken not to damage the fragile gold layer. Wires

Fig. 5. PCB DSC solar panel prototype board, ready for integration with sensor node, the DSC module is $50\text{ mm} \times 50\text{ mm}$

were soldered onto the board such that the entire module could be used or individual cells could be measured and/or bypassed if faulty. Figure 4 shows the PCB that serves as the base for the new solar cell. The board, which is composed of four copper stripes each 49 mm wide and 6 mm long, was manufactured using a milling machine from an Eagle CAD design. In the next version of this prototype board, a modern maximum power point tracker (MPPT) will be integrated in the system. By using a MPPT, the cell's power output can be increased up to 15-20% [26].

Figure 5 shows a board produced with a DSC on a PCB. The module created was tested before and after integration with the PCB, using alligator clips to make the electrical connections for tests prior to the connection to the PCB was made, with wires soldered to the PCB used after connection. The module was also tested 5 months after construction. During storage the cell was placed in a drawer in ambient atmosphere and generally in the dark.

VI. EXPERIMENTAL SETUP

Several experiments were performed to investigate the performance of the PCB-based cell. To evaluate the performance of the module under standard conditions a solar simulator was used. The modules were tested under 1 Sun illumination, 100 mWcm^{-2} AM1.5G, using a 1000 W solar simulator xenon lamp (Oriol) fitted with an appropriate filter to achieve spectral match and a Keithley 2400 source meter. Illumination intensity was varied by the use of fine wire mesh and calibrated using a silicon diode. The active area was 10.5 cm^2 , while the size of the glass was 25 cm^2 , this shows a poor active area to device area ratio. In future work will attempt to increased this to over 90% coverage, as a challenging, yet achievable, target for an interconnected module of this size. No masking was used; efficiencies may therefore be over estimated due to light piping within the glass.

To investigate the real world performance and feasibility for practical use, tests were performed both indoors and outdoors using different light sources.

A. Measurement system

A measurement system was created to capture characterization measurements for the PCB solar cell. The measurement system, shown in Figure 6, consists of a 24-bit analog-to-digital converter (ADC) that measures the voltage drop over a 5Ω resistor, which is used to measure current. To obtain an I-V curve, a digitally programmable potentiometer was also used so that different loads could be presented to the cell. A Mulle v3.1 networked sensor node equipped with a Bluetooth 2.0 transceiver was connected to the measurement system. Using this approach, the PCB cell can be tested outdoors by having a wireless connection to a laptop or PC, which can be placed indoors. The measurement system will be used also to measure the temperature dependency of the cell during winter tests. In addition, the measurement system also serves as a building block in the power supply unit (PSU) that may be used together with the PCB-cell. The PSU includes a boost converter that generates a 5.0V output used to charge a super capacitor. A switch is used to select whether the Mulle should be powered by the super capacitor or by a battery. The Mulle v3.1 also features a battery monitor chip, capable

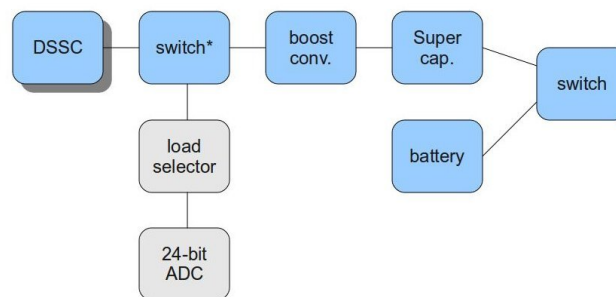


Fig. 6. Measurement system overview

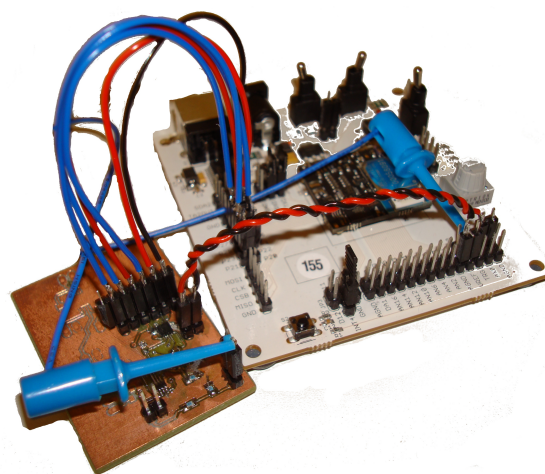


Fig. 7. Measurement system implementation

of measuring battery voltage, power consumption, available energy, and estimated lifetime. Combined with the Mulle's on-board features, the PSU can enable true energy- and power-aware operation.

Figure 6 shows the measurement system. The system can measure voltages up to 6.5V, and current with a resolution around $20\mu\text{A}$. The load can be programmed to any value between 100Ω and $100\text{k}\Omega$ in 256 steps. Its realisation is shown in Figure 7.

The measurement system is completely wireless, which allows remote monitoring of the PCB cell. A dedicated software written in C was used to retrieve data from the Mulle and store the results to file on a computer.

B. Performed measurements

The following experiments were performed in order to test the cell's performance under in a real-world setting. The different tests that the cell was tested in are typical application locations where a networked embedded system can be deployed.

TABLE I
MULLE v3.1 CURRENT CONSUMPTION

Mode	Delay	Current
All systems sleep	-	0.004 mA
MCU 10.0 MHz, BT off	-	7.6 ma
MCU 5.0 MHz, BT off	-	5.1 mA
MCU 2.5 MHz, BT off	-	3.1 mA
MCU 1.25 MHz, BT off	-	2.2 mA
MCU sleep, BT listen	2-12 s.	1.0 mA
MCU sleep, BT active	-	40.3 mA
MCU sleep, BT sniff (210 slots)	131 ms.	8.4 mA
MCU sleep, BT sniff (2010 slots)	1256 ms.	2.8 mA
MCU sleep, BT parked (18 slots)	13 ms.	7.5 mA
MCU sleep, BT parked (200 slots)	130 ms.	2.7 mA
MCU sleep, BT parked (4094 slots)	2560 ms.	1.8 mA

- 1) Measurement of the PCB DSC module's performance initially and after 5 months
- 2) Measurement of the PCB DSC's current response at various light incident angles
- 3) Measurement of the effect of varying light intensity on the current output of the PCB DSC module.
- 4) Tests of power generation at indoor and outdoor locations and different lighting conditions

The cell was tested for long term degradation effects and different light sources at different angles. However, no temperature tests were performed during the work.

C. Real-world energy usage

The feasibility of using the prototype solar cell, with the power characteristics presented in the previous section, for a real-world networked sensor is presented here. The Mulle node [27] has been used in a number of WSN and BSN applications [28], which will be used as an example for calculating operational lifetimes when combined with the PCB cell. Table I shows examples of the current consumption of a Mulle v3.1 in different operating modes.

VII. RESULTS

The initial performance of the PCB DSC module was 1.4% prior to integration with the PCB, and was improved to 1.5% after integration. The performance degraded to approximately 1% after 5 months, as shown in Figure 8. It can be seen that integration with the PCB has improved device performance by increasing the short circuit current,

although this could be partially explained by a change in the testing methodology, brought about by how the module is placed under the light beam due to the bulky PCB causing the device to be placed in a slightly different position in the light beam. The improvement in the electrical connection of the module to the testing apparatus by connection to the PCB would also account for some of the improvement, with sections not previously in electrical connection due to breaks or scratches in the gold layer being connected via the PCB. It is also possible that the increase in current is due to reflection from the metal surfaces associated with integration with the PCB. The overall device performance is not high, but as a prototype solid-state module it has sufficient performance to be a starting point for considering future applications. Over the course of 5 months it can be seen that the performance of the DSC module decreased by about 30%, which is quite good for a DSC with no encapsulation and stored under open circuit conditions in ambient atmosphere. The short circuit current reduction over the time was most likely due to the degradation of the dye molecules through interaction with atmospheric water, which may also explain the reduced fill factor as the water will have also degraded the Spiro-MeOTAD thus increasing series resistance.

Varying illumination angle was performed by the use of a rotating stage with a 360° protractor attached to its center to determine the angle. The modules were attached to the center of the freely rotating protractor and a mark on the board was used to determine the incident angle, where 0° corresponds to the light beam from the solar simulator being perpendicular to the surface of the module. A spirit level was used to determine when the modules were perpendicular to the light beam and all other angles were calculated from this calibration. From the data in Figure 9 the DSC module appears to have a reasonably low angular dependence, following the cosine law [29], where the cosine of the angle of illumination predicts the fraction of current being produced compared to perpendicular for collimated light sources such as the sun, due to its distance, or nominally the solar simulator. Comparing the experimental results with the cosine law shows that the currents produced are higher than expected for the DSC module. Possible reasons for this are, as the modules were rotated half approaches the light source, if the light beam is not properly collimated

then the light will have higher intensity for the closer portion and thus the current will increase, alternatively it could be due to light piping effects through the glass from the edge of the device (4 mm) playing a role in capturing more light into the device. The important point to take from this experiment is that at 45° the DSC still produced about 80% output current, which shows for most of a given day the DSC will be performing with relatively good output regardless of the angle of incidence of solar illumination. The silicon module follows the theoretical curve more closely until around 60°, where it begin to perform below the curve. The comparison of these devices shows that the DSC has a lower angular dependence than the silicon module tested here, thus demonstrating a possible advantage for this technology for use in sensor nodes.

Figure 10 shows the variation of the output current with varied input light intensity, which remains linear for lower light intensities, but slightly decreases upon approaching full illumination, showing the cell is approaching it's photocurrent limit. This limiting would not be an issue for real world applications where the input light intensity would generally be lower than the standard 1 sun considered here, and in the context of Mulle sensor nodes then times of peak light intensity will typically be uninteresting as the device should have had the opportunity to fully charge by the time this level of irradiation is present. Meaning that the device will likely be charged during the morning before the peak light of the day in an outdoor application. This data may also be used to estimate the illumination intensity from the photocurrent produced by the module although this will exhibit a significant spectral mismatch for artificial light sources.

To evaluate the module's output in real world scenarios the short circuit current was measured at a number of locations that reflect typical applications for the sensor node which can be placed either outdoors or indoors.

The resulting data is in Table III. For a number of practical usage scenarios assuming no real-time radio communication, a small dye solar cell should be sufficient to provide the necessary power for making low-cost wireless power a reality.

When comparing the current output from the PCB DSC cell with Table I, it is clear that the generated current is sufficient for powering a Mulle sensor

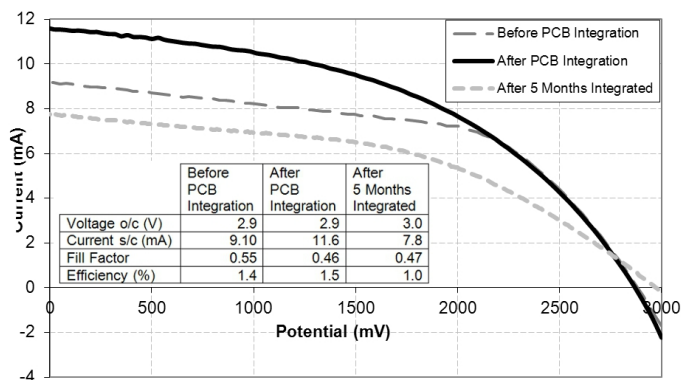


Fig. 8. PCB DSC current-voltage performance, initially and after 5 months

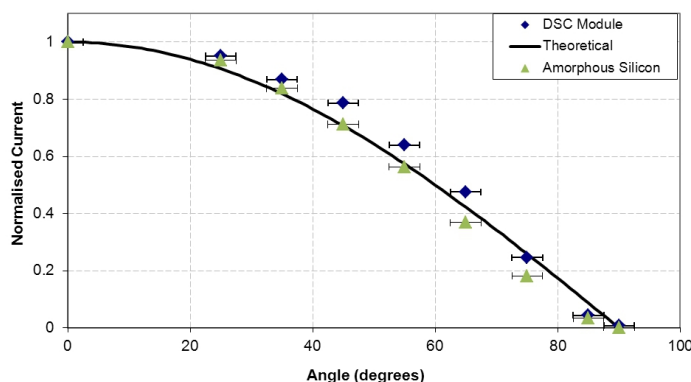


Fig. 9. PCB DSC short circuit current response for different light incident angles

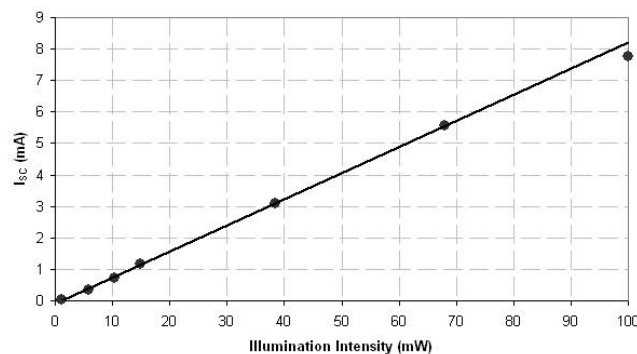


Fig. 10. Short circuit current response for the PCB DSC with light intensity varying between 1 and 100%

node as long as low-power modes are utilized. Since the peak power of a Mulle is higher than the maximum power output of the PCB DSC cell, some energy storage will always be required. A super capacitor, a rechargeable battery, or a combination of both can be used for energy storage. Performed

TABLE II
TEST LOCATIONS

ID	Description
1	Office with ceiling fluorescence lightning and ambient light from shaded windows; cell horizontal
2	Corridor with ceiling fluorescence lightning and no ambient light from windows, cell horizontal
3	Workshop well lit with with ceiling fluorescence lightning and some ambient light from shaded windows; cell horizontal
4	Office desk with 23W desk fluorescent lamp; cell horizontal
5	Near a closed window with no direct sunlight; cell horizontal
6	Near an open window with no direct sunlight; cell horizontal
7	Near a closed window with some direct sunlight; cell horizontal
8	Near a closed window with direct sunlight; cell horizontal
9	Near a closed window with no direct sunlight; cell tilted for maximum illumination
10	Outside in full sun light; cell horizontal
11	Outside in full sun light; cell tilted for maximum illumination

TABLE III
CURRENTS FROM PCB DYE SOLAR CELL IN TYPICAL USAGE
SCENARIO LOCATIONS.

Test location	distance to source [m]	Current [μA]
1	2	6
1	0.3	60
1	0.1	220
2	1	6
2	0.1	90
3	2	50
4	0.2	240
4	0.01	3000
5	-	220
6	-	330
7	-	800
8	-	2650
9	-	3700
10	-	6800
11	-	8000

tests indicates that the presented approach is feasible for powering low-power electronics such as sensor nodes.

VIII. CONCLUSION AND FUTURE WORK

This paper has presented a novel approach for powering low-power electronic devices, such as networked embedded systems and sensor nodes. The approach integrates a dye sensitised solar cell directly onto a device's circuit board thereby reducing the material and assembly costs. A prototype device has been manufactured to demonstrate the

feasibility of this approach and to enable the cells' real-world performance to be evaluated. Test results, both initial and after five months of degradation, have been presented to support the claims. Note that the performed tests only show the feasibility of the system, more tests are needed in order to fully characterize the cell's true performance.

By integrating the power supply directly onto a circuit board, the authors envision that networked sensors may be manufactured at a greatly reduced cost in the future. When combined with new technologies for energy storage and transparent encapsulation, the presented approach can be an enabling technology for future low-cost, large-scale wireless sensor networks, in support of the vision of *the Internet of Things*.

The first steps towards an integrated manufacturing process for solar-powered embedded systems have been successfully completed. The authors are now working on techniques to print a dye sensitised solar cell directly onto a printed circuit board using mass production techniques. The ultimate aim is to develop a method for assembling and manufacturing a complete system that includes a PCB, components, and a solar cell, using a single process.

Another issue that needs further investigation is how the system should be encapsulated in a transparent package. One method is to embed the entire system in optically transparent glue, as shown in [30]. How low temperatures are affecting the cell's performance must also be investigated. Finally, the use of a more low powered device, such as the Mulle v5.2 with an IEEE 802.15.4 radio, combined with a maximum power point tracker (MPPT) should be used to test the true performance in a wireless sensor and actuator network used in for example ITS applications, e-Health or smart homes.

ACKNOWLEDGMENTS

Parts of this work have been conducted within the iRoad project that is hosted at Luleå University of Technology. Funding provided by Geveko ITS A/S, the Gunnar och Märtha Bergendahl foundation and VINNOVA are hereby gratefully acknowledged. The authors would like to thank Mikael Larsson for help with the manufacturing of the circuit boards.

REFERENCES

- [1] J. Eliasson, J. Delsing, S. Thompson, and Y.-B. Cheng, "PCB Integration of Dye-sensitized Solar Cells for Low-cost Networked Embedded Systems," in *SENSORCOMM*, Nice, France, July 2011.
- [2] D. Culler, D. Estrin, and M. Srivastava, "Overview of sensor networks," *Computer*, vol. 37, no. 8, pp. 41–49, Aug 2004.
- [3] Özgür B. Akan and I. F. Akyildiz, "Event-to-sink reliable transport in wireless sensor networks," *IEEE/ACM Trans. Netw.*, vol. 13, no. 5, pp. 1003–1016, 2005.
- [4] T. Bokareva, W. Hu, S. Kanhere, B. Ristic, N. Gordon, T. Bessell, M. Rutten, and S. Jha, "Wireless sensor networks for battlefield surveillance," 2006. [Online]. Available: <http://www.cse.unsw.edu.au/~tbokareva/papers/lwc.html>
- [5] N. Xu, S. Rangwala, K. K. Chintalapudi, D. Ganesan, A. Broad, R. Govindan, and D. Estrin, "A wireless sensor network for structural monitoring," in *SenSys '04: Proceedings of the 2nd international conference on Embedded networked sensor systems*. New York, NY, USA: ACM, 2004, pp. 13–24.
- [6] A. Mainwaring, D. Culler, J. Polastre, R. Szewczyk, and J. Anderson, "Wireless sensor networks for habitat monitoring," in *Proceedings of the 1st ACM international workshop on Wireless sensor networks and applications*. ACM Press, 2002, pp. 88–97.
- [7] "IPSO Alliance," <http://www.ipso-alliance.org/>, 2010, [Online; accessed 11-June-2012].
- [8] L. Atzori, A. Iera, and G. Morabito, "The internet of things: A survey," *Comput. Netw.*, vol. 54, no. 15, pp. 2787–2805, Oct. 2010. [Online]. Available: <http://dx.doi.org/10.1016/j.comnet.2010.05.010>
- [9] K. Zeng, K. Ren, W. Lou, and P. J. Moran, "Energy aware efficient geographic routing in lossy wireless sensor networks with environmental energy supply," *Wireless Networks*, vol. 15, pp. 39–51, Jan 2009.
- [10] R. Moghe, Y. Yang, F. Lambert, and D. Divan, "A scoping study of electric and magnetic field energy harvesting for wireless sensor networks in power system applications," in *Energy Conversion Congress and Exposition, 2009. ECCE 2009. IEEE*, sept. 2009, pp. 3550–3557.
- [11] V. Raghunathan, A. Kansal, J. Hsu, J. Friedman, and M. Srivastava, "Design considerations for solar energy harvesting wireless embedded systems," *IPSN '05: Proceedings of the 4th international symposium on Information processing in sensor networks*, vol. 64, p. 64, 2005, cited By (since 1996): 9. [Online]. Available: www.scopus.com
- [12] J. Eliasson, P. Lindgren, J. Delsing, S. Thompson, and Y.-B. Cheng, "A power management architecture for sensor nodes," in *Wireless Communications and Networking Conference, 2007.WCNC 2007. IEEE*, march 2007, pp. 3008–3013.
- [13] E. Blackshear, M. Cases, E. Klink, and S. Engle, "The evolution of build-up package technology and its design challenges," *IBM journal of research and development*, vol. 49, pp. 641–661, 2005.
- [14] B. O'Regan and M. Grätzel, "A low-cost, high-efficiency solar cell based on dye-sensitized colloidal TiO_2 films," *Nature*, vol. 353, no. 6346, pp. 737–740, 1991.
- [15] B. A. Gregg and M. C. Hanna, "Comparing organic to inorganic photovoltaic cells: Theory, experiment, and simulation," *Journal of Applied Physics*, vol. 93, no. 6, pp. 3605–3614, 2003. [Online]. Available: <http://link.aip.org/link/?JAP/93/3605/1>
- [16] M. A. Green, K. Emery, Y. Hishikawa, and W. Warta, "Short Communication Solar cell efficiency tables," *Progress in Photovoltaics: Research and Applications*, vol. 17, 2009.
- [17] M. A. U. Usman, "Integrating dye-sensitized solar cell technology for implementation in modern day electronics," in *SOLAR 2010 Conference Proceedings*, Piscataway, NJ 08855-1331, United States, 2010.
- [18] R. Hostettler, W. Birk, and M. Nordenvaad, "Feasibility of road vibrations-based vehicle property sensing," *Intelligent Transport Systems, IET*, vol. 4, no. 4, pp. 356–364, December 2010.
- [19] "The iRoad project," <http://www.iroad.se>, April 2011, [Online; accessed 19-May-2012].
- [20] A. Dohr, R. Modre-Opsrian, M. Drobnics, D. Hayn, and G. Schreier, "The internet of things for ambient assisted living," in *Information Technology: New Generations (ITNG), 2010 Seventh International Conference on*, april 2010, pp. 804–809.
- [21] O. Asad, M. Erol-Kantarci, and H. Mouftah, "Sensor network web services for demand-side energy management applications in the smart grid," in *Consumer Communications and Networking Conference (CCNC), 2011 IEEE*, jan. 2011, pp. 1176–1180.
- [22] N.-H. Nguyen, Q.-T. Tran, J.-M. Leger, and T.-P. Vuong, "A real-time control using wireless sensor network for intelligent energy management system in buildings," in *Environmental Energy and Structural Monitoring Systems (EESMS), 2010 IEEE Workshop on*, sept. 2010, pp. 87–92.
- [23] L. Han, A. Fukui, N. Fuke, N. Koide, and R. Yamanaka, "High efficiency of dye-sensitized solar cell and module," in *IEEE 4th World Conference on Photovoltaic Energy Conversion*. IEEE, 2006, pp. 179–182.
- [24] U. Bach, D. Lupo, P. Comte, J. E. Moser, F. Weissortel, J. Salbeck, H. Spreitzer, and M. Grätzel, "Solid-state dye-sensitized mesoporous TiO_2 solar cells with high photon-to-electron conversion efficiencies," *Nature*, vol. 395, pp. 583–588, 2009.
- [25] J. Burschka, A. Dualch, F. Kessler, E. Baranoff, N.-L. Cevey-Ha, C. Yi, M. K. Nazeeruddin, and M. Grätzel, "Tris(2-(1H-pyrazol-1-yl)pyridine)cobalt(III) as p-type dopant for organic semiconductors and its application in highly efficient solid-state dye-sensitized solar cells," *Journal of the American Chemical Society*, vol. 133, no. 45, pp. 18042–18045, 2011. [Online]. Available: <http://pubs.acs.org/doi/abs/10.1021/ja207367t>
- [26] F. Simjee and P. Chou, "Efficient charging of supercapacitors for extended lifetime of wireless sensor nodes," *Power Electronics, IEEE Transactions on*, vol. 23, no. 3, pp. 1526–1536, may 2008.
- [27] "Eistec AB," <http://www.eistec.se>, 2010, [Online; accessed 11-June-2012].
- [28] J. Eliasson, P. Lindgren, and J. Delsing, "A Bluetooth-based Sensor Node for Low-Power Ad Hoc Networks," *Journal of Computers (JCP)*, pp. 1–10, May 2008.
- [29] J. Balenzategui and F. Chenlo, "Measurement and analysis of angular response of bare and encapsulated silicon solar cells," *Solar Energy Materials and Solar Cells*, vol. 86, no. 1, pp. 53–83, 2005. [Online]. Available: <http://www.sciencedirect.com/science/article/pii/S092702480400265X>
- [30] J. Eliasson and W. Birk, "Towards road surface monitoring: Experiments and technical challenges," in *Control Applications, (CCA) Intelligent Control, (ISIC), 2009 IEEE*, july 2009, pp. 655–659.